AD-A265 622

CUMENTATION PAGE

OMB No 0704 0188

(2)

2. REPORT DATE	3. REPORT TYPE AND DATES COVERED
27 May 1993	Technical 5/92-5/93

4. TITLE AND SUBTITLE
Nonlinear Optical Spectroscopy of Ag(111) in Electrolyte and in Vacuum

5. FUNDING NUMBERS
ONR N00014089-J-1261

6. AUTHOR(S)
R. Bradley, R. Georgiadis, S. D. Kevan, and G. L. Richmond

7. PERFORMING ORGANIZATION NAME(S) AND ADDRESS(ES)
Department of Chemistry
University of Oregon
Eugene, OR 97403

8. PERFORMING ORGANIZATION REPORT NUMBER
ONR Technical Report # 2

9. SPONSORING/MONITORING AGENCY NAME(S) AND ADDRESS(ES)
Office of Naval Research
Chemistry Program
800 North Quincy Street
Arlington, VA 22217-5000

10. SPONSORING/MONITORING AGENCY REPORT NUMBER

11. SUPPLEMENTARY NOTES

12a. DISTRIBUTION/AVAILABILITY STATEMENT
Approved for public release: distribution unlimited

12b. DISTRIBUTION CODE

13. ABSTRACT *(Maximum 200 words)*

In this paper, we investigate the electronic structure of a metal surface in the presence of aqueous electrolyte and an applied potential by optical second harmonic generation (SHG). We have obtained the detailed wavelength dependence (λ_{SH} =300-350 nm) of the SH response from Ag(111) in both an aqueous electrolyte and in ultrahigh vacuum (UHV) and find that, when the Ag(111) electrode is biased at the potential of zero charge (PZC), the SH response is strongly correlated with the SH response in UHV. For the surface in both environments there is a sharp peak near 3.82 eV. Possible contributing factors to this peak are discussed. In the electrochemical environment, the effect of applied potential on the SH response at longer wavelengths, (nonresonant regime), is consistent both with previous observations at fixed frequencies and predictions of the surface charge density (SCD) model. At resonant wavelengths, there is a dramatic deviation from behavior predicted by the SCD model, a result consistent with previous experiments at discrete wavelengths.

14. SUBJECT TERMS
Ag(111) electrode surfaces; resonant optical second harmonic generation; electronic structure

15. NUMBER OF PAGES
43

16. PRICE CODE

17. SECURITY CLASSIFICATION OF REPORT	18. SECURITY CLASSIFICATION OF THIS PAGE	19. SECURITY CLASSIFICATION OF ABSTRACT	20. LIMITATION OF ABSTRACT
UNCLASSIFIED	UNCLASSIFIED	UNCLASSIFIED	

OFFICE OF NAVAL RESEARCH

Grant N00014-89-J-1261

R&T Code 4131038

Technical Report No. 2

"Nonlinear Optical Spectroscopy of Ag(111) in Electrolyte and in Vacuum"

by

R. Bradley, R. Georgiadis, S.D. Kevan and G.L. Richmond

Submitted to J. Chem. Phys.

Department of Chemistry
University of Oregon
Eugene, OR 97403

May 1993

TECHNICAL REPORT DISTRIBUTION LIST - GENERAL

Office of Naval Research (2)*
Chemistry Division, Code 1113
800 North Quincy Street
Arlington, Virginia 22217-5000
ATTN: DR PETER SCHMIDT

Dr. James S. Murday (1)
Chemistry Division, Code 6100
Naval Research Laboratory
Washington, D.C. 20375-5000

Dr. Robert Green, Director (1)
Chemistry Division, Code 385
Naval Air Weapons Center
Weapons Division
China Lake, CA 93555-6001

Dr. Elek Lindner (1)
Naval Command, Control and Ocean
Surveillance Center
RDT&E Division
San Diego, CA 92152-5000

Dr. Bernard E. Douda (1)
Crane Division
Naval Surface Warfare Center
Crane, Indiana 47522-5000

Dr. Richard W. Drisko (1)
Naval Civil Engineering
Laboratory
Code L52
Port Hueneme, CA 93043

Dr. Harold H. Singerman (1)
Naval Surface Warfare Center
Carderock Division Detachment
Annapolis, MD 21402-1198

Dr. Eugene C. Fischer (1)
Code 2840
Naval Surface Warfare Center
Carderock Division Detachment
Annapolis, MD 21402-1198

Defense Technical Information
Center (2)
Building 5, Cameron Station
Alexandria, VA 22314

* Number of copies to forward

NONLINEAR OPTICAL SPECTROSCOPY OF THE AG(111) SURFACE IN AN ELECTROLYTE AND IN VACUUM

R. A. Bradley†, R. Georgiadis*, S. D. Kevan†† and G. L. Richmond

Department of Chemistry

and

††Department of Physics
University of Oregon
Eugene, OR 97403

ABSTRACT

In this paper, we investigate the electronic structure of a metal surface in the presence of aqueous electrolyte and an applied potential by optical second harmonic generation (SHG). We have obtained the detailed wavelength dependence (λ_{SH} = 300-350 nm) of the SH response from Ag(111) in both an aqueous electrolyte and in ultrahigh vacuum (UHV) and find that, when the Ag(111) electrode is biased at the potential of zero charge (PZC), the SH response is strongly correlated with the SH response in UHV. For the surface in both environments there is a sharp peak near 3.82 eV. Possible contributing factors to this peak are discussed. In the electrochemical environment, the effect of applied potential on the SH response at longer wavelengths, (nonresonant regime), is consistent both with previous observations at fixed frequencies and predictions of the surface charge density (SCD) model. At resonant wavelengths, there is a dramatic deviation from behavior predicted by the SCD model, a result consistent with previous experiments at discrete wavelengths.

current addresses: †Molecular Science Research Center, Pacific Northwest Laboratory, Richland, Washington, 99352.
*Department of Chemistry, George Washington University Washington , D.C. 20052

I. INTRODUCTION

Over the past decade, our understanding of the electronic structure of metal surfaces examined under UHV conditions has improved significantly, aided by the proliferation of powerful electron spectroscopic techniques. Unfortunately, parallel elucidation of the detailed surface electronic structure at the metal/electrolyte interface has not followed suit, largely because of the lack of suitable techniques for making comparable measurements in-situ. This lag is understandable if one considers the difficulties, both theoretical and experimental, in treating the metal/electrolyte interface. The experimental requirements are quite daunting, since experimental techniques suited to this environment must be capable of distinguishing the electronic structure of the surface from that contributed from the bulk metal, without being hampered either by the presence of the electrolyte or the large field gradient at the surface.

The paucity of detailed electronic structure information for surfaces in solution raises important questions and controversies. What correlation if any exists between the electronic structure of surfaces in solution and the electronic structure measured in UHV? Perhaps more important to electrochemists, how do the electronic properties of the metal surface vary with the applied potential? Since the surface electronic structure of clean surfaces in UHV can be extremely sensitive to the presence of even submonolayer amounts of adsorbates, the contended persistence of surface states in the presence of aqueous electrolyte often receives skepticism. Intrinsic surface states and surface modified continuum bands, both consequences of the truncation of the periodic crystal lattice, are often invoked in investigations of optical properties of metals in solution. However, without compelling and unambiguous experimental confirmation these assignments are speculative, particularly when extended to extrinsic surface states induced by the presence of defects, adsorbates or the applied field.

In this paper we have used surface second harmonic generation (SHG) as a probe of the electronic properties of a metal surface immersed in solution and under the control of

an applied potential. This nonlinear optical technique holds particular promise for studies of buried interfaces because of the inherent surface specificity and because of its versatility for studying surfaces in a variety of environments.[1, 2] The main emphasis of our study involves obtaining the detailed wavelength dependent measurements of the SH response from the Ag(111) surface in solution and performing comparative SH measurements of the surface in UHV. This direct correlation between surface electronic structure for a metal both in solution and in UHV has not previously been demonstrated by any single technique. In addition to simply monitoring the SH intensity as a function of wavelength, the rotational anisotropy in the SH response as the crystal is rotated azimuthally is also measured at several wavelengths. Whereas simple wavelength dependent scans demonstrate how the SH *intensity* can describe a resonance between surface electronic bands at either the incident wavelength (λ,) and the SH wavelength (λ_{SH}), rotational anisotropy measurements also contain information about the relative *phase* of the response. Our studies show that as a resonance is approached, it is reflected not only in the intensity, but in the relative phase of the response and leads to dramatic variations in the SH rotational anisotropy with incident wavelength. For Ag(111) we find a resonance near 3.82 eV which is present for the metal in both UHV and in an electrolyte solution where the bias is held at the potential of zero charge (PZC). The possible factors contributing to this response including surface electronic structure and bulk dielectric properties of the metal are discussed.

A second emphasis of this work is an investigation of the potential dependence of the SH response in an attempt to understand how the surface electronic properties vary with applied potential. We have limited our study to the ideally polarizable potential region to avoid charge transfer reactions at the interface. Under such charging conditions, we find that the SH response reflects perturbations arising not only from a change in the surface excess charge density but also from the modification of the surface electronic structure of the metal. We have isolated these effects through prudent selection of both the optical

polarization conditions and the excitation wavelength.

II. EXPERIMENTAL

For the optical measurements at 1064 nm and 532 nm excitation, the fundamental or SH output from a 10 Hz Nd:YAG laser producing 10 ns pulses was used. The output of a Nd:YAG pumped dye laser was employed for other visible and near IR wavelengths. The effective angle of incidence for both the UHV and solution experiments described here was fixed at 30^{o}. High extinction coefficient broadband polarizing beamsplitting cubes selected the polarization of the light striking the metal surface and the SH light generated at the surface. For the dye laser experiments, a portion of the incident light was split off from the main beam and directed through a 1 mm long quartz cell containing a suspension of KDP powder in decahydronapthalene. The transmitted SH light served as a non-linear reference[3] to normalize for the quadratic dependence of SHG and to correct for intensity variations in the dye laser gain curve. Appropriate filters and a monochromator separate the second harmonic signal (or reference) from the specularly reflected (or transmitted) fundamental light. The output of each monochromator was detected by a photomultiplier tube using a fast preamplifier and gated electronics.

For both experiments, the 99.999% pure Ag(111) crystal (Monocrystals, Cleveland, OH) were oriented within 1^{o} by Laue X-ray diffraction and mechanically polished with diamond paste to 1 μm. For the UHV experiments, the surface was etched with chromic acid before insertion into UHV. After successive cycles of sputtering and annealing to 400^{o} C, the Ag(111) surface was found free of impurities by Auger and exhibited a LEED pattern characteristic of a well ordered (1x1) surface. For the solution experiments, the mechanically polished surface was maintained under an inert, O_2 free atmosphere throughout the electrochemical polishing and subsequent transfer into the electrochemical cell. All solutions were prepared from high purity salts and Nanopure water and were continuously purged with oxygen free N_2 during the experiments to avoid oxide formation. The electrochemical cell used for these studies has been described previously[4].

All potentials for the electrochemical studies are referenced to the Ag/AgCl electrode.

III. THEORY

A. SHG from fcc metals

In centrosymmetric media such as fcc silver, SHG is forbidden under the electric dipole approximation in the bulk, but allowed at the metal surface where inversion symmetry is broken. Because of this broken centrosymmetry, the surface dipole susceptibility elements χ_{ijk} that describe this SHG process are particularly sensitive to the surface and it's associated electronic properties. The relationship between the dispersion of the tensor elements of $\chi^{(2)}$ and the electronic band structure can be described in single-particle excitation picture by the following equation,

$$\chi^{(2)}_{ijk}(2\omega;\ \omega,\ \omega) = -Ne^3 \sum_{(a,b,c)} \frac{\langle a | r_i | c \rangle \langle c | r_j | b \rangle \langle b | r_k | a \rangle}{(2\hbar\omega - E_{ca} - i\hbar\gamma_{ca})(\hbar\omega - E_{ba} - i\hbar\gamma_{ba})} \qquad (1)$$

where r_i is the cartesian coordinate operator, and $|a\rangle$, $|b\rangle$, and $|c\rangle$ represent the initial, intermediate and upper state, respectively. When either the fundamental or SH photon energy approaches the energy of an optical transition between two single particle states, χ_{ijk} may be resonantly enhanced and the resulting signal will differ from the nonresonant case in both phase and intensity. The presence or absence of a resonance is further constrained by the matrix elements in the numerator, which are determined by the symmetry selection rules for coupling two single particle states with the optical field.

For wavelength dependent studies of single crystal metal surfaces, the azimuthal dependence of the response may be exploited to measure the dispersion in the intensity and phase of individual components contributing to overall surface response. Based on phenomenological models developed by Tom[5] and Sipe[6], tthe azimuthal dependence of the dipole allowed SH response from a (111) surface can be described by the following expressions for the polarization combinations used in our studies:

$$I_{p,p}^{(2\omega)}(\phi) \propto \left| \begin{array}{c} F_z\chi_{zzz}f_zf_z + F_z\chi_{zxx}f_xf_x + F_x\chi_{xzx}f_zf_x \\ +F_x\chi_{xxx}f_xf_x\cos(3\phi) \end{array} \right|^2 \quad (2)$$

$$I_{p,s}^{(2\omega)}(\phi) \propto \left| F_y\chi_{yxx}f_xf_x\sin(3\phi) \right|^2 \quad (3)$$

$$I_{s,p}^{(2\omega)}(\phi) \propto \left| F_z\chi_{zyy}f_yf_y + F_x\chi_{xyy}f_yf_y\cos(3\phi) \right|^2 \quad (4)$$

$$I_{m,s}^{(2\omega)}(\phi) \propto \left| F_y\chi_{yxy}f_zf_y + F_y\chi_{yxy}f_zf_y\cos(3\phi) \right|^2 \quad (5)$$

where f_i and F_i are the Fresnel coefficients for the fundamental and harmonic fields. The intensity subscripts refer to the polarizations of the fundamental and SH light, respectively. For Equation 5, m refers to mixed polarization comprised of 50% p and 50% s polarization. The azimuthal angle ϕ is defined as the angle between the $[2\bar{1}\bar{1}]$ direction and the projection of the incident wavevector parallel to the surface. Terms in the above expressions which explicitly contain angular dependence are referred to as anisotropic terms with the coefficients proceeding the sine or cosine term represented by $c^{(3)}$ (Eq. 2, 4 and 5) and $b^{(3)}$ (Eq. 3). For each polarization, the remaining isotropic terms are represented by $a^{(\infty)}$.

Most of the SHG measurements presented in this work are obtained with p-polarized fundamental light and either p- or s-polarized second harmonic light. For p-input and p-output (p, p) polarization the observed intensity modulation with azimuthal rotation, or rotational anisotropy, arises from the interference between $c^{(3)}$ and $a^{(\infty)}$. A best fit of such data to Equation 2 yields the ratio of these terms, $c^{(3)}/a^{(\infty)}$, which contains a magnitude and phase angle reflecting the extent of the interference under the given experimental conditions. Therefore, rotational anisotropy under (p, p) polarization conditions is very sensitive to relative changes in both magnitude and phase of either the isotropic or anisotropic contributions. It is important to note that for media with complex dielectric constants such as silver, not only the susceptibility elements but the Fresnel

coefficients will influence this interference.

An expression for the induced polarization in the medium, $\mathbf{P}_{eff}^{(2)}$, including both surface and bulk contributions is the following[7]:

$$\mathbf{P}_{eff}^{(2)}(2\omega) = \vec{\vec{\chi}}^{D}:\mathbf{E}(\omega)\mathbf{E}(\omega) + \vec{\vec{\chi}}^{P}:\mathbf{E}(\omega)\nabla\mathbf{E}(\omega) - \nabla\vec{\vec{\chi}}^{Q}:\mathbf{E}(\omega)\mathbf{E}(\omega)$$
$$-\vec{\vec{\chi}}^{Q}:\nabla\mathbf{E}(\omega)\mathbf{E}(\omega) + \frac{c}{i2\omega}\nabla\times[\vec{\vec{\chi}}^{M}:\mathbf{E}(\omega)\mathbf{E}(\omega)] \qquad (6)$$

The first two terms are electric dipole in nature, the third and fourth describe the electric quadrupole contribution and the last term is the magnetic dipole contribution. The first and third terms originate from the surface whereas the others are bulk in nature. Although surface contributions to the SH response from the magnetic dipole source term have been observed[8], they should not be a factor in the studies presented here and are neglected.

When interpreting an SH response which displays surface sensitivity, the dipolar terms are most important relative to the multipole terms that involve gradients in both the optical fields and the quadrupolar susceptibility. For the anisotropic response this omission is justified as the tangential components of the optical field are continuous and the multipole contribution (the third term in Equation 6) to this response is not surface sensitive. In contrast, the isotropic response may contain additional multipole contributions that are sensitive to the gradient normal to the surface, and this can significantly complicate the analysis of this response.[7] For these reasons, caution must be practiced when using phase and intensity changes in the SH response to locate surface resonances. For most optical polarization schemes, the response arises from an interference involving a number of tensor elements each having an associated magnitude and phase. When the azimuthal angle is fixed at $\phi = 30^0$, appropriate polarization conditions can be used to separate the different contributions to the response. For example, p-in and s-out polarization isolates the in-plane, or anisotropic, response contained in the coefficient $b^{(3)}$ (and $c^{(3)}$) arising from the susceptibility elements χ_{xxx} (=- χ_{xyy} = - χ_{yxy}= - χ_{yxx}), the dipolar response, and ζ, the quadrupolar response. Under p-in and p-out polarization one can isolate the $a^{(\infty)}$ term,

which is referred to as isotropic since the involved susceptibility elements do not vary with azimuthal angle. This out-of-plane response contains the surface dipolar terms χ_{zxx} ($= \chi_{zyy}$), χ_{xzx}($= \chi_{yyz}$), and χ_{zzz} as well as possible contributions from higher order susceptibility terms that can have both surface and bulk contributions.

B. Potential dependence of the SH response

In the presence of an applied field, the following expression[9] has been used to describe the additional third order hyperpolarizibility induced by the dc field at the interface:

$$I^{(2\omega)}(\vec{E}_{dc}) \propto \left| P_0^{(2\omega)} + P_1^{(2\omega)}(\vec{E}_{dc}) \right|^2 \tag{7}$$

Here the total SH signal as a function of applied potential arises from both a potential independent nonlinear polarization $P_0^{(2\omega)}$,which is the usual expression, as well as a potential dependent nonlinear polarization $P_1^{(2\omega)}$, which is described by the following:

$$P_1^{(2\omega)}(\vec{E}_{dc}) = \gamma \vec{E}_{dc}\left(\vec{E}(\omega) \bullet \vec{E}(\omega)\right) + \gamma' \vec{E}(\omega)\left(\vec{E}_{dc} \bullet \vec{E}(\omega)\right) \tag{8}$$

where $\vec{E}_{dc}$ is the static electric field oriented normal to the surface and γ, γ' are material constants. As written, Equation 8 is only valid for electric fields perpendicular to the surface and explicitly assumes that χ_{zzz} dominates the potential dependent SH response.

More recently, the Surface Charge Density (SCD) model[10-12] has been used to explain potential dependence observed in the SH response from metal electrodes. In this model, Gauss's law was used to express the potential dependence of the SH response in terms of the excess surface charge density on the electrode. Since the difference in the normal component of the light across the metal-electrolyte interface is proportional to the surface charge density, the charging behavior in this SH response can be described in a four wave mixing formalism by the second and fourth terms in Equation 6. However, it is important to note that the tangential component of the light is continuous, making this mechanism unable to explain any potential dependence of the in-plane response (under p-input and s-output polarization) and only the first term of Equation 6 contributes to the

surface response. This characteristic of the in-plane response will be exploited in the analysis of the electrochemical measurements, as the only interpretation available for any charging behavior observed is changes in the dipolar susceptibility element χ_{yxx}.

IV. RESULTS

A. UHV studies

Figure 1(a) shows the explicit wavelength dependence of the normalized SH intensity from Ag(111) in UHV for p-in and s-out (p,s) polarization from λ_{SH} = 307 nm to λ_{SH} = 375 nm. The normalized intensity shows a sharp peak at λ_{SH} = 325 nm (3.82 eV), with a FWHM of 100 meV. Figure 1(b) shows the corresponding measurement of the normalized SH intensity from Ag(111) in UHV for p-in and p-out (p,p) polarization. No peak is observed in this case and the intensity at lower energy appears featureless. The significantly lower overall intensity and different spectral dependence of Figure 1(b) relative to Figure 1(a) suggests that the susceptibility elements that contribute to this response are probing different surface features than the χ_{yxx} dipolar tensor element that is monitored in Figure 1(a).

The dispersion seen in the two wavelength scans of Figure 1 are entirely consistent with anisotropy data at discrete wavelengths in this wavelength region. The anisotropy measurements, however, contain additional information about the relative phase between $a^{(\infty)}$ and $c^{(3)}$. Shown in Figures 2(a-d) are rotational anisotropy measurements under (p,p) polarization conditions for Ag(111) in UHV at the following four frequencies: λ_{SH} = 532 nm, 320 nm, 305 nm, and 266 nm. The progression from six peaks at λ_{SH} = 532 nm to three peaks at λ_{SH} = 266 nm in the rotational anisotropies is best described by a change in the relative phase angle (between $a^{(\infty)}$ and $c^{(3)}$) from $\pi/2$ to 0 degrees. Data collected for additional wavelengths (not shown) indicate that the largest part of the relative phase angle change occurs near λ_{SH} = 320 nm, the same spectral region as the peak seen in Figure 1(a). This is strong complementary evidence for a resonance and demonstrates the correlation

between relative phase angle changes in rotational anisotropy measurements and the existence of a resonance peak in intensity scans. We find that the anisotropies are a much easier means of identifying a resonance initially. The intensity scans result in gradual intensity changes and require significant effort to normalize the response over a several laser dyes.

Figure 3 shows the explicit wavelength dependence of the normalized SH intensity from Ag(111) in UHV for s-in and p-out (s,p) polarization (at $\phi = 30^{o}$) from $\lambda_{SH} = 315$ nm to $\lambda_{SH} = 337$ nm. Under these polarization conditions, the tensor element χ_{zzz} is accessed and shows no discernible features in this spectrum.

B. Solution studies

Analogous wavelength dependent SH measurements were also obtained in the electrochemical cell containing 0.1 M $NaClO_4$ electrolyte. Figures 4(a-c) show the normalized SH intensity from Ag(111) at three applied potentials for p-in and s-out (p,s) polarization from $\lambda_{SH} = 307$ nm to $\lambda_{SH} = 375$ nm. For Figure 4(b), the crystal was biased at -0.7 V (PZC) to minimize the charging effects from the dc field across the electrochemical interface. Similar to the measurement in UHV, the normalized intensity shows a peak at $\lambda_{SH} = 325$ nm (3.82 eV), with a comparable FWHM. This surprising qualitative agreement implies that *at the PZC*, the peak observed in UHV is not strongly perturbed by the presence of the electrolyte. Although normalized intensity values for the UHV (Fig 1(a)) and electrochemical measurements are not directly comparable due to power density differences, the qualitative agreement between the spectra is striking. Comparison of the rotational anisotropies from Ag(111) in UHV and in 0.1 M $NaClO_4$ electrolyte, biased at the PZC, for a variety of wavelengths extending from the infrared through the visible also shows the same striking similarity[13]. This resemblance is significant because dramatic changes have been observed in the anisotropies[14] when the crystal is biased away from the PZC for all wavelengths studied.

The SH wavelength scans for (p,s) polarization demonstrate the sensitivity of this

peak to electrode charging. Figure 4(a) reveals that when the crystal is biased positive of the PZC (-0.2 V), the intensity of the peak is attenuated whereas application of a potential negative of the PZC (-1.2 V) results in an increase in the peak intensity (Fig. 4(c)). For the sake of clarity, the spectra will be separated into two regions: near the peak (3.6 to 4.0 eV, $\lambda_{SH} \geq 345$ nm) will be referred to as the resonant region and the spectral region away from the peak (3.2 to 3.6 eV, $\lambda_{SH} \leq 345$ nm) as the nonresonant region. Two observations are particularly noteworthy. First, the peak intensity is very sensitive to the charging of the interface, but this charging does not cause an energetic shift (stark shift) in the peak position. Second, in the nonresonant spectral region of both Figures 4(a) and 4(c) there is a negligible charging effect compared to that of the peak, as observed previously for the nonresonant SH response with (p,s) polarization at 1064 nm[14].

To model the data of Figures 1(a) and 4(a-c) in terms of associated optical transitions, both the imaginary part of the susceptibility associated with the oscillator strength of these transitions and the dispersive contribution from the real part of $\chi^{(2)}$ must be included. To do this we extend Andermann's model to describe the real and imaginary parts of the second order susceptibility in terms of a damped harmonic oscillator[15]. In this model multiple resonances are incorporated into a description of the dielectric function by including a summation over bands. A least squares fit to the data using this model is shown as the solid line in Figures 1(a) and 4(a-c). Only one resonance was necessary to accurately fit the data. The imaginary part of χ_{yxx}, proportional to the joint density of states (JDOS), was derived and the resulting relative magnitude of $\mathrm{Im}(\chi_{yxx})$ plotted against the applied potential (Fig. 5). $\mathrm{Im}(\chi_{yxx})$ decreases in a linear fashion with the applied potential with an x-intercept of +1.1 V. The implications of this plot will be discussed in a later section.

Figures 6(a-c) shows the explicit wavelength dependence of the normalized SH intensity from Ag(111) in 0.1 M $NaClO_4$ electrolyte for (p,p) polarization from $\lambda_{SH} = 307$ nm to $\lambda_{SH} = 375$ nm, with the curves as a guide to the eye. For the measurements shown in

Figure 6(b), the crystal was biased at the PZC. The intensities in Figure 1(a) and 4(b) were set equal and the measurements under (p,p) polarization were scaled appropriately, allowing a qualitative comparison between Figures 6(b) (PZC) and 1(b) (UHV) to be made. As in UHV, no peak was observed and the intensity in the nonresonant region also appears relatively dispersionless and of similar magnitude to the UHV response. The solution results demonstrate that the (p,p) polarized SH response is sensitive to changes in the surface charging as the applied potential is varied, although the largest intensity change occurs in the nonresonant portion of the spectrum in contrast to the behavior seen in Figures 4(a,c) for the s-polarized output. When the crystal is biased positive of the PZC (-0.2 V), Figure 6(a), the intensity in the nonresonant portion of the spectrum increases, whereas for charging negative of the PZC (-1.2 V), Figure 6(c), very little change in the intensity results. This charging behavior is opposite to that observed under (p,s) polarization conditions, where positive charging decreases the peak intensity. The charging behavior in the nonresonant portion of Figures 6(a,c) is entirely consistent with what has been previously observed at longer wavelengths[12, 16]. In contrast, the resonant portion of the (p,p) polarized spectra are relatively insensitive to electrode charging.

To determine which isotropic tensor elements contribute to the charging effect seen in Figures 6(a,c), rotational anisotropy measurements were performed under nonresonant conditions. Figures 7(a,b) show the strong charging effect on the rotational anisotropy measurements from Ag(111) in 0.1 M $NaClO_4$ electrolyte for (m,s) polarization under nonresonant conditions at λ_{SH} = 360 nm, with the curve representing a fit to a function similar to Equation 5. Under this polarization condition, only one isotropic dipolar tensor element (χ_{xzx}) is accessed and its potential dependence can be isolated. Under these nonresonant conditions, the contribution from this term is small at the PZC, Figure 7(a), and clearly increases with positive charging, as seen in Figure 7(b).

V. DISCUSSION

A. Electronic Resonances

One of the most striking results of this work is that in solution, we find that the nonlinear optical properties (and corresponding electronic properties) of the surface biased *at the PZC* remain unaltered by the presence of electrolyte over a wide spectral range, as seen by comparing Figures 1(a,b) to Figures 4(b), 6(b). The presence of electrolyte imparts no spectral shift on the peak position, a result also supported by the remarkable similarity between SH anisotropy data for Ag(111) in UHV and at the PZC (in a nonspecifically adsorbing electrolyte) under a wide variety of incident frequencies[13].

The presence of an applied field at potentials away from the PZC has a significant effect on the surface properties as manifested by changes in the nonlinear optical response in both the resonant and nonresonant regimes. Since the Thomas-Fermi screening length in a metal is of the order of one atomic layer, the applied potential is rapidly screened at the surface. For nonresonant wavelengths, the potential dependence of the nonlinear optical response varies in a manner consistent[10-12] with the SCD model. For resonant wavelengths, the observed charging behavior is opposite to that seen for nonresonant wavelengths and cannot be described by the SCD model. The peak intensity dramatically changes as the surface is charged away from the PZC. This behavior is particularly evident in rotational anisotropy scans taken at wavelengths where λ_{SH} is near the peak. For a change of +500 mV from the PZC, the relative phase increases by 63°, which leads to very different anisotropy patterns[14]. The fact that we observe such a strong potential dependence of the peak, Figures 4(a-c), implies that the peak has significant contributions from the surface region. It is interesting that this potential dependence appears under (p,s) polarization, where χ_{yxx} is a factor. Currently, no simple mechanism exists to account for the coupling of the applied field (in the z direction) to the in-plane χ_{yxx} susceptibility.

Since our results for Ag(111) at the PZC are identical to the UHV measurements, we view the charging behavior of the surface in solution as a perturbation of the electronic properties of the metal as they exist in UHV. As discussed below, there are several

mechanisms by which this could occur, one originating at the surface which would be consistent with the potential dependence of the response as discussed above, and the others of a bulk nature.

1. Surface Electronic Structure

The surface electronic structure of Ag(111) in UHV has been determined in UHV by several studies. In particular, angle resolved photoemission measurements[17, 18] have identified a surface electronic state located 120 meV below the Fermi level at $\bar{\Gamma}$ in the surface Brillouin zone. This occupied state of Λ_1 symmetry, which we will refer to as A, has a very narrow natural linewidth estimated to be less than 50 meV. Unoccupied surface electronic states, attributed to an image potential state, I, has also been reported near $\bar{\Gamma}$ on Ag(111). This feature is located in an allowed region of the projected bulk electronic structure near the top of the s-p band gap, ~3.75 eV above the Fermi level and has been observed by several groups [19, 20] using k-parallel resolved inverse photoemission spectroscopy. Bulk states which might be involved are the occupied sp band and the d-bands as well as the unoccupied sp band.

Appropriate optical selection rules and detailed polarization dependent studies can be helpful in assigning which electronic structure features may contribute to our observed peak. For example, for the experimental polarization conditions under which the peak is observed (p,s) only input and output photons of E_x or E_y polarization can couple to the observed transition. The ability to apply an electric field to the surface in the electrochemical cell provides an additional variable for elucidating the surface states and bands involved in the resonance. The effect of the field is determined by the spatial profile of the state or band in question in the near surface region where the applied field is screened by the metal.

Surface state A is a plausible initial state for a resonant transition since it is spatially localized to the surface. Since it lies very close to the Fermi level, its energetic position relative to the bulk states and its occupation should be sensitive to an applied potential. In a manner analogous to the work function, the electrochemical potential will increase as the

metal is charged positively because more work must be done to extract electrons from the Fermi level. Thus the bulk bands in the metal will be shifted to higher binding energy (relative to E_{vac}) under conditions of positive charging, but surface localized bands or states will shift less and move to a lower binding energy relative to the bulk bands as they experience some fraction of the applied potential. For state **A**, positive charging will lead to depopulation of the state as its energy is shifted above the electrochemical potential[21]. For negative charging, state **A** will shift further below the electrochemical potential and increase in occupation. This is consistent with the intensity changes we observe, assuming that any energetic shift is small relative to the peak width. At positive potentials, Figure 4(a), the peak intensity drops, consistent with the depopulation of **A**. For negative charging, the reverse would be expected and is observed in Figure 4(c). Additional support for the possible role of A in the resonance feature comes from polarization experiments. With the initial state being surface state A (of Λ_1 symmetry), dipole selection rules for χ_{yxx} require that the upper state has Λ_3 symmetry. Such a transition should not only be observable in χ_{yxx}, but should also be found in the dispersion of χ_{xzx} since the dipole selection rules for a two photon resonance are the same for both tensor elements. To isolate χ_{xzx}, we use mixed input polarization (50% p-in and 50% s-in) and s-out polarization (at $\phi = 30^{o}$). Under these conditions, a peak is observed. The fact that the peak is not seen under (p,p) polarization conditions, where χ_{zxx}, χ_{xzx}, and χ_{zzz} may contribute, is likely due to an interference between contributing terms.

Evidence gained from the electrochemical experiments that the surface state **A** is the initial state of the two photon resonance must be corroborated by examining the surface sensitivity of the peak observed in UHV. The peak shown in Figure 1(a) exhibits a considerable surface sensitivity to both alkali adsorbates and temperature[22], but neither spectrally shifts nor completely disappears. Linear reflectivity measurements have shown[23, 24] that the interband transitions for Ag are sensitive to temperature. In fact, the previously observed temperature dependence of the SH response from Ag(110) in UHV at

λ_{SH} = 320 nm[25] was attributed to a bulk interband transition, although the authors note that a SH response that couples to surface electronic structure should also be sensitive to temperature. The observed temperature dependence of the peak in Fig 1(a) has a different slope than that observed from Ag(110) surface, but this does not rule out a bulk component in our response. However, the sensitivity of the peak in Figure 1(a) to alkali adsorption implies that the peak contains a significant contribution from the surface which we attributed to the surface state A as the initial state of the two photon resonance seen in the dipolar term χ_{yxx}. Overall, our UHV measurements suggest that although a significant portion of the SH signal arises from the surface, there exists some contribution to the peak intensity that arises from a spatial region not perturbed by surface modifications, namely a bulk contribution that may contribute through either a quadrupolar contribution or the Fresnel coefficients. These contributions will be discussed later.

Our results from Ag(111) in UHV (Fig. 1), can be compared directly with the previous studies of Giesen et al.[26] in which a similar peak was found in wavelength dependent SH intensity measuremens of Ag(111) in UHV. Their work was conducted with only the input polarization specified, possibly accessing all tensor elements under p-input whereas for s-input polarization, both χ_{zxx} and χ_{yxx} could contribute. They assigned the SH peak to the **A-I** transition, basing their assignment on their two-photon photoemission measurements which also showed a sharp resonance feature at 3.84 eV which they attributed to a one photon resonance between two states of Λ_1 symmetry: the occupied crystal induced surface state **A** and the unoccupied (n = 1) image potential state **I**. Their SH results were entirely consistent with the two-photon photoemission assignment since the susceptibility elements χ_{zzz} and χ_{zxx} are allowed for a two photon resonance between states of Λ_1 symmetry. The assignment is however not consistent with our observation of a resonance in χ_{yxx} which is found using p,s polarization. The selection rules for χ_{yxx} require that the upper state in the two-photon resonance in the SH experiments is of a different symmetry than the intermediate state in the photemission

experiment. If the upper state were of Λ_1 symmetry, as concluded by Giesen et. al.,[26] then a two-photon resonance should also be seen in χ_{zxx} as well as χ_{zzz}. As shown in Figure 3, careful measurements of the SH dispersion (proportional to $|f_z f_x \chi_{zxx} F_x|^2$) under (s,p) polarization conditions show no evidence of such a resonance. Furthermore, we would expect the image potential state **I** to shift in energy with applied potential with respect to the bulk bands, but by a different amount than the occupied surface state **A** as it has a different spatial profile and is centered further away from the metal, into the electrolyte. This implies that a two photon resonance between states **A** and **I** in solution should spectrally shift with applied potential, a prediction not observed in Figures 4(a-c).

The most likely upper transition level would be the unoccupied bulk band edge. Along the $\overline{\Sigma}$ symmetry line the wavefunctions comprising the s-p bands (and associated surface states) have Λ_1 symmetry, making a two photon resonance forbidden under the selection rules for χ_{yxx}. However, at points off the $\overline{\Sigma}$ line, the two photon resonance between surface state **A** and the unoccupied bulk band edge is not constrained by selection rules and is allowed for all polarizations. Since the fraction of transitions which occur along $\overline{\Sigma}$ is vanishingly small, the two photon transition essentially integrates the joint density of states between the lower and upper bands. However, the absence of a resonance in Figure 3 under (s,p) polarization is difficult to reconcile with the allowed nature of the two photon resonance. It is plausible that an interference between either the Fresnel coefficient or a bulk quadrupolar response and the surface dipolar χ_{zxx} masks the resonance feature. In the surface region where the applied potential is screened, the bulk band edge and the surface state **A** can have a similar spatial profile and thus may energetically shift by a similar amount with applied potential. This predicted dependence is more consistent with the behavior observed for the peak in solution.

Two previous studies have examined the electronic structure of Ag(111) in solution by linear (ER) and nonlinear electroreflectance. In an ER study,Schneider et al.[27] reported two spectral features at 3.5 eV and 4.0 eV, both observed only when the crystal was biased

negative of the PZC. They attributed the sharp feature at 3.5 eV to the **A-I** transition, invoking electrolyte and potential effects to account for the discrepancy with the UHV value for this transition energy 3.8 eV. They based their assignment of the initial state on inverse photoemission measurements performed in UHV[28] which incorrectly placed the energetic position of **A** at 400 meV above the Fermi level at $\bar{\Gamma}$ rather that 120 meV below the Fermi level as determined by photoemission[17, 18] and inverse photoemission[19] studies. A broad feature near 4.0 eV was assigned to a transition from the surface state **A** to the unoccupied bulk sp band edge. Both of these features in the ER spectra showed no noticeable shift in their energetic position with potential. The authors assign the final state **I** of this transition based on Giesen's two-photon photoemission measurements[26], which implies that the initial state **A** must be at least partially occupied in UHV. For this to be consistent with the energetic position determined by Reihl[28] then state **A** must have a width in UHV on the order of 400 meV, which is not borne out by later photoemission measurements[18].

In more recent nonlinear electroreflectance measurements, Furtak et al.[29] examined the *isotropic* (p,p) SH response from Ag(111) over a range of SH photon energies from 2.8 eV to 4.46 eV, normalizing at each wavelength the potential dependent SH response with the magnitude of the SH response observed at the PZC. In qualitative agreement with the results of Figures 6(a,b) under nonresonant conditions, they found for positive charging that the SH response behaved in a manner consistent with the SH studies from polycrystalline silver[30]. They attributed a spectral feature near 3.4 eV to the above mentioned A-I transition (coupling to χ_{zzz}) and invoked the arguments of Schneider et al.[27] to rationalize the appearance of the feature *only* under negative charging. These results are in stark contrast to the spectra shown in Figures 6(a,c), where little, if any charging effect is observed and no peak is observed at or near 3.4 eV. However, it is possible that this discrepancy is due the different incidence angle in our experiments disfavoring a possible coupling to χ_{zzz}.

It is clear from our studies that if surface electronic structure plays a role, the peak

\at 3.82 eV which we assigned to a transition between A and the unoccupied bulk band edge, is energetically unaltered in the presence of the solution when the potential is biased at the PZC. This implies that the surface state A is occupied at the PZC, as well as in UHV, and has a narrow linewidth in solution. If the energy shifts upward by more than 120 mV or the state spreads significantly due to the presence of electrolyte, the spectral profile of the peak would be altered from that observed in UHV. These results are more in agreement with the 50 meV limit set by the ARPES measurements[18] for surface state A than with the ~400 mV width assumed in both the ER and the nonlinear ER work. Further, the striking similarity in the anisotropy measurements[13] and intensity measurements from the Ag(111) surface in solution at the PZC and in UHV are not consistent with arguments requiring the state A to be unoccupied at the PZC, the assumption critical to the assignment of the features in the ER spectra.

2. *Influence of Fresnel Factors*

In addition to a surface electronic structure contribution, one must also consider that the peak in the SH spectra could be a simple result of the bulk dielectric properties of the metal. Since the dielectric constant of silver has structure in the spectral region near 3.8 eV, only the Fresnel coefficient for the radiated SH light, F_y, and not the Fresnel coefficient at the fundamental wavelength, f_x, will reflect this structure. As plotted in Figure 8, we calculated wavelength dependence of the Fresnel coefficients for the radiated SH light, F_z , F_k and F_z, for our optical geometry using Mizrahi's model[31] and the values for the silver dielectric constants as obtained from Johnson and Christy[32]. As should be expected, all three Fresnel coefficients exhibit structure near 3.8 eV due to the interband transitions of Ag.

From Equation 4, we note that the s,p polarized spectra in Figure 3 (at $\phi = 30$) is proportional to $\left|F_z\chi_{zyy}f_yf_y\right|^2$, the dipolar surface response. A comparison of the plot of F_z and the spectrally flat Figure 3 suggests that the tensor element χ_{zyy} may have a spectral

dependence similar to the (p,s) polarized data that is masked by an interference between the Fresnel coefficient and the tensor element. Under p,s polarization conditions, the Fresnel coefficient F_z (F_y in crystal coordinates) will influence the spectral dependence and exhibits one similar to the SH response measured in UHV (Fig. 1) and in surface in solution biased at the PZC.(Fig. 4 (b)). The width of the peak in the SH spectrum in Figure 1 is narrower than the plotted Fresnel coefficient F_z, suggesting a contribution from the tensor element χ_{yxx}. However, the strongest evidence for an interpretation involving χ_{yxx} comes from the potential dependence of the peak, Figures 4 (a-c), which cannot be successfully described by the Fresnel model as it treats the surface as a boundary condition.

Nevertheless, the Fresnel model shows a qualitative agreement with the dispersion of the SH response and is thus likely contributing. The primary difficulty with this model is that it provides no clear mechanism for a potential dependence of χ_{yxx} since the Fresnel theory only treats the fields in the bulk of the material. One might simply argue that as the potential is varied, the surface electronic density is modified which changes the screening of the intraband transitions at the surface. In this scenario, this lead to an alteration of the intensity of the peak without perturbing the peak, which is dominated by the Fresnel factors. However, at longer wavelengths no such charging *in the in-plane response* χ_{yxx} has been observed[14] making this scenario only speculation since one cannot prove such an interpretation.

3. Bulk Quadrupolar Contribution

The quadrupolar terms in Equation 6 may contribute to the SH response in this spectral region for silver, but under p-in and s-out polarization they are not surface sensitive on the (111) surface. Recent experimental studies by Furtak and coworkers have shown that on Ag(100) these quadrupolar terms do not contribute in this spectral region as manifested in the absence of observable anisotropy.[29] Furthermore, as discussed in Section III, under these polarization conditions the four wave mixing process similar to that

described by the SCD model cannot be a factor and the only mechanism available to describe potential dependence in this SH response is changes in the *dipolar* tensor element χ_{xxx}. For these reasons, we will treat the observed potential dependence solely as a perturbation of the *surface* electronic dipolar susceptibility χ_{yxx}.

4 Modelling the Potential Dependence

The strong potential dependence observed in the intensity and phase of the SH response from the Ag(111) electrode under resonant conditions is a clear indication that the electronic properties of the surface region must be included in any model describing the potential dependence. Whereas the simplest approach might seem to be to model it in terms of Fresnel theory, Fresnel theory treats the interface as a boundary condition and only describes the linear fields in the bulk of the material. Thus, changes in the surface properties cannot be included. For understanding how this potential dependence might be viewed in terms of alteration of electronic structure, we provide the following simple model.

Since the surface electronic structure at the PZC appears from experiments to be unaltered from that observed in UHV[13], we use the known energetics of surface state A in UHV and assume similar surface properties for state A at the PZC, placing it 120 meV below ε_f. Assuming that the peak intensity is proportional to the occupancy of the surface state A, Figure 5 yields a potential dependence for surface state A of 0.06 eV/Volt. The plot also suggests that at +1.1 V the initial state of any two photon resonance should become completely depopulated.

To describe this perturbation of the surface electronic structure induced by variation of the applied potential (work function), we have adapted the model of Weinert, Hulbert, and Johnson[33] (WHJ) pertaining to the metal-vacuum interface. In this model the surface state wavefunctions in the interfacial region are separated into three regions and the binding energy of the states are found as a function of the image plane position, an adjustable

parameter of the model. For Ag(111) in vacuum, this model gives good agreement with the observed binding energies for the n = 0, 1, 2 surface states in UHV for a choice of the image plane position of z_{im} = 0.21 atomic units outside the jellium edge[33]. To model the effect of this applied potential, we simply shift the bulk electronic structure (and associated parameters for the surface state wavefunctions) by the magnitude of the voltage bias away from the PZC and calculate the energetic shift of the n = 0 surface state, our candidate for the initial state of the two photon resonance. The justification for this approach is found in emersion studies[34] which established a one–to–one correspondence between changes in the applied potential in solution and work function changes in UHV.

Figure 9 contains the results of this calculation in which the binding energy of the n = 0 surface state is determined as a function of the image plane position for three applied potentials. As a reasonable starting point, we fix the image plane position at the WHJ value of 0.21 a.u. and examine the energetics of A as a function of applied potential. At the PZC (-0.7 V), the calculated curve for the binding energy (BE) yields BE =30 meV with respect to ε_f and reproduces the curve previously calculated for Ag(111) in UHV[35]. With positive charging (+0.5 V from the PZC), the state is shifted to lower BE and becomes depopulated, whereas with negative charging (-0.5 V from the PZC), the state is shifted to higher BE and becomes increasingly occupied. From the curves in Fig. 9, the shift of the n = 0 surface state (A) with applied potential is calculated to be 0.12 eV/V. Considering the simplicity of the model, this value is in reasonable agreement with the shift derived from Figure 5 . The shift is too small to be observed in our experiments, consistent with the lack of energetic shift in the resonant peak as a function of potential.(Fig. 4(a-c)) It is important to mention that the magnitude of the stark shift of surface state A derived from Figure 5 will be larger if there is an underlying bulk contribution to the peak position or intensity, but it should be more in line with our simple calculation rather than the large shifts seen in the ER measurements.[29, 36]

The trends in our results are in agreement with calculations of the screening of an

external field at the Ag(100) surface performed by Aers and Ingelsfield using the surface embedding method[37]. This modeling involved calculating the electronic structure of Ag(100) in the absence and presence of the field, and measuring the *shift* in the center of gravity of the screened charge with the field and thus the perturbation of the surface electronic structure. To compare with electroreflectance measurements on this surface, they examined three surface states and found, for field strengths comparable to those used in our study, stark shifts of 0.05, 0.125, and 0.325 eV/V, with the magnitude dependent on the spatial extent of state's charge density. This modeling fell short of explaining the large stark shifts observed in the ER measurements on this surface and Aers and Ingelsfield concluded that large local field effects were needed to explain the experimental ER results on Ag(100) if they were due to surface states.

B. Nonresonant Response

Theoretical descriptions of the potential dependence of the SH response have been limited to treating the metal electrode as free electron-like within the jellium model.[29, 36] Experimentally, one observes a strong potential dependence at positive potentials and weaker effect at negative potentials[10-12]. The potential dependence of the normal component of the SH response is modeled by inducing a static uniform electric field oriented perpendicular to the surface and recalculating the nonlinear response of the system in the presence of this field. While significant progress has been made with such jellium approaches in descriptions of the incident angle and applied potential dependence of the SH signal[30, 38-40], even under nonresonant conditions, there are serious deficiencies in describing other experimental observations. The usual assumption made is that the in-plane nonlinear polarization, Rudnick and Stern's $b(\omega)$, is constant and thus potential independent. Both Guyot-Sionnest et al.[30] and Furtak et al.[29] modeled the potential dependent SH response completely in terms of Rudnick and Stern's $a(\omega)$ (the out-of-plane nonlinear polarization) neglecting terms other than the potential dependent part of χ_{zzz} ,

which we will refer to as γ_{zzzz}.

Our experiments suggest that one cannot assume $b(\omega)$ to be potential independent. To show this, we isolate the potential dependence of the tensor elements comprising the isotropic response through rotational anisotropy measurements corresponding to (p,p), (m,s), and (s,p) polarizations. In this analysis, the bulk contributions are neglected and each of the isotropic dipolar tensor elements χ_{ijk} is assumed to be independent of applied potential and any observed potential dependence is described by a real γ_{ijlk}, in a manner similar to Eqs.7 and 8. As the dipolar χ_{ijk} are assumed to be potential independent, the only source of potential dependence results from γ_{ijlk}. By collecting the anisotropy data for these three polarizations at two different potentials, -0.2 V and -0.7 V(PZC), a ratio corresponding to the potential dependence in the isotropic response can be extracted. For the (m,s) and (s,p) polarizations, this a value proportional to the potential dependent part of the dipolar susceptibility:

$$r_{in,out} = \frac{\left|F_i\left(\chi_{ijk} + \gamma_{ijlk}\right) f_j f_k\right|}{\left|F_i\left(\chi_{ijk}\right) f_j f_k\right|} \tag{9}$$

where γ_{ijlk} effectively describes the potential dependence of the second order dipolar susceptibility χ_{ijk}. The expression for (p,p) polarization is more complicated than for (s,p) and (m,s), since it involves three isotropic terms[41], but it can be easily constructed from Equation 8. For (s,p) polarization in the nonresonant portion of the spectra, λ_{SH} = 360 nm, no measurable potential dependence ($r_{s,p} \approx 1$) is observed, suggesting that both χ_{zxx} and γ_{zxzx} are small under our experimental conditions. For (m,s) polarization measurements (Figures 7(a,b)), $r_{m,s}$ = 1.8, demonstrating that the in-plane nonlinear polarization is indeed strongly potential dependent and should not be neglected. Similar measurements under (p,p) polarization exhibit a strong potential dependence, with $r_{p,p}$ = 1.79. Whereas this might suggest that a large portion of the potential dependence in the

(p,p) response is due to χ_{xzx} and γ_{xzzx}, its relative contribution is not easily determined as it depends on the incidence angle (through the Fresnel coefficients) as well as the relative phase between χ_{xzx}, χ_{zxx} and χ_{zzz}.

VI. CONCLUSIONS

This study demonstrates the value of direct comparative measurements for correlating electronic properties in solution with the known electronic properties of metals in UHV. The trend observed in the relative phase (obtained by fitting the rotational anisotropies) is consistent with the existence of a resonance condition and with the detailed wavelength dependent measurements. A resonant transition at 3.82 eV observed in UHV and in solution remains unperturbed by the presence of the electrolyte at the PZC and correlates well with the known electronic structure in UHV. The results are discussed in terms of contributions from surface electronic structure and bulk dielectric properties of the metal. Charging the interface away from the PZC affects this resonance through changes in the electronic properties of the metal. A simple model is proposed for explaining the potential dependence in surface electronic structure at this metal surface.

The SH response we observe under nonresonant conditions is consistent with the existing models of coupling to the surface excess charge density. However, we find, contrary to what has been assumed in many studies, that the nonlinear (SH) current induced in the plane of the surface, χ_{xzx}, is indeed quite sensitive to the charging of the interface. More importantly for the electrochemical community and the study of Ag electronic structure in solution, our results reveal the striking similarity in the nonlinear optical response from Ag in UHV and solution, when the Ag electrode is held at the PZC.

Acknowledgments

The authors wish to thank both Dr. Andreas Friedrich and Dr. E.K.L. Wong for scientific discussions pertaining to the manuscript. Financial support from the National

Science Foundation (FAW 9022538 and CHE 8801348) and the Petroleum Research Fund of the American Chemical Society is gratefully acknowledged.

References

1. Richmond, G.L., Robinson, J.M. and Shannon, V.L., Prog. in Surf. Sci., **28**, 1 (1988).
2. Shen, Y.R., Nature, **337**, 519 (1989).
3. Jones, R.D. and Callis, P.R., J. Appl. Phys., **64**, 4301 (1988).
4. Koos, D.A., Shannon, V.L. and Richmond, G.L., J. Phys. Chem., **94**, 2091 (1990).
5. Tom, H.W.K., *Ph.D. Dissertation* University of California, Berkeley,(1984).
6. Sipe, J.E., Moss, D.J. and van Driel, H.M., Phys Rev. B, **35**, 1129 (1987).
7. Guyot-Sionnest, P. and Shen, Y.R., Phys. Rev. B, **38**, 7985 (1988).
8. Reif, J., Zink, J.C., Schneider, C.M. and Kirschner, J., Phys. Rev. Lett., **67**, 2878 (1991).
9. Lee, C.H., Chang, R.K. and Bloembergen, N., Phys. Rev. Lett., **18**, 167 (1967).
10. Corn, R.M., Romagnoli, M., Levenson, M.D. and Philpott, M.R., Chem. Phys. Lett., **106**, 30 (1984).
11. Corn, R.M., Romagnoli, M., Levenson, M.D. and Philpott, M.R., J. Chem. Phys., **81**, 4127 (1984).
12. Rojhantalab, H.M. and Richmond, G.L., J. Phys. Chem., **93**, 3269 (1989).
13. Bradley, R.A., Georgiadis, R., Kevan, S.D. and Richmond, G.L., J. Vac. Sci. Tech. A, **10**, 2996 (1992).
14. Georgiadis, R. and Richmond, G.L., J. Phys. Chem., **95**, 2895 (1991).
15. Andermann, G., A.Caron and Dows, D.A., J. Opt. Soc. Am., **55**, 1210 (1965).
16. Koos, D.A., *Ph. D Dissertation* University of Oregon,(1991).
17. Roloff, H.F. and Neddermeyer, H., Solid State Commun., **21**, 561 (1977).
18. Kevan, S.D. and Gaylord, R.H., Phys. Rev. B, **36**, 5809 (1987).
19. Hulbert, S.L., Johnson, P.D., Stoffel, N.G. and Smith, N.V., Phys. Rev. B, **32**, 3451 (1985).
20. Altmann, W., Dose, V. and Goldmann, A., Z. Phys. B Condensed Matter, **65**, 171 (1986).
21. In our discussion, we refer to the electrochemical potential as $(V_b + \varepsilon_f)$ where ε_f is the *kinetic Fermi energy* and remains unperturbed by charging of the interface and V_b is the Volta potential describing the coulombic interaction of the electrons with the positive ion cores. Whereas some studies in the literature call ε_f the electrochemical potential, this is not strictly correct. (See S. Trasatti, The Electrode Potential, in "Comprehensive Treatise of Electrochemistry", Ed. J.O'M. Bockris, B.E. Conway, and E. Yeager, Plenum Press, New York 1980.)

22. Bradley, R.A., *Ph.D. Dissertation* University of Oregon,(1992).

23. Rosei, R., Culp, C.H. and Weaver, J.H., Phys. Rev. B, **10**, 484 (1974).

24. Rosei, R., Phys. Rev. B, **10**, 474 (1974).

25. Hicks, J.M., Urbach, L.E., Plummer, E.W. and Dai, H.L., Phys. Rev. Lett., **61**, 2588 (1988).

26. Giesen, K., Hage, F., Riess, H.J., Steinmann, W., Haight, R., Beigang, R., Dreyfus, R., Avouris, P. and Himpsel, F.J., Physica Scripta, **35**, 578 (1986).

27. Schneider, J., Franke, C. and Kolb, D.M., Surf.Sci., **198**, 277 (1988).

28. Reihl, B., Frank, K.H. and Otto, A., Z. Phys. B., **62**, 473 (1986).

29. Furtak, T.E., Simpson, L.J. and Tang, Y., Phys. Rev. B, **46**, 1719 (1992).

30. Guyot-Sionnest, P., Tadjeddine, A. and Liebsch, A., Phys. Rev. Lett., **64**, 1678 (1990).

31. Mizrahi, V. and Sipe, J.E., J. Opt. Soc. Am. B, **5**, 660 (1988).

32. Johnson, P.B. and Christy, R.W., Phys. Rev. B, **6**, 4370 (1972).

33. Weinert, M., Hulbert, S.L. and Johnson, P.D., Phys. Rev. Lett., **55**, 2055 (1985).

34. Rath, D.L. and Kolb, D.M., Surf. Sci., **109**, 641 (1981).

35. There is a slight discrepancy between our value and the one that WHJ found for the n = 0 surface state of Ag(111) in UHV, but this is probably due to slightly different choices of the bulk parameters for the Goodwin wavefunctions.

36. Franke, C., Piazza, G. and Kolb, D.M., Electrochim. Acta, **34**, 67 (1989).

37. Aers, G.C. and Inglesfield, J.E., Surf. Sci., **217**, 367 (1989).

38. Chang, R.K. and Bloembergen, N., Phys. Rev., **144**, 775 (1966).

39. Brown, F., Parks, R.E. and Sleeper, A.M., Phys. Rev. Lett., **14**, 1029 (1965).

40. Murphy, R., Yeganeh, M., Song, K.J. and Plummer, E.W., Phys. Rev. Lett., **63**, 318 (1989).

41. Caution must be exercised when using information obtained under (m,s) and (s,p) polarizations to interpret the relative contributions under (p,p) polarization, as not only will the Fresnel coefficients be different, but the different isotropic contributions may interfere in the (p,p) polarized SH response.

May 20, 1993

FIGURE CAPTIONS

Figure 1. (a) Wavelength dependence of the normalized SH intensity from Ag(111) (ϕ = 30°) in UHV for p-in and s-out (p,s) polarization as a function of the second harmonic photon wavelength in nm (lower axis) and energy in eV (upper axis). The solid curve shown for each data set is a least squares fit to the Anderman model. (see text). (b) Analogous SH measurement from Ag(111) (ϕ = 30°) in UHV for p-in and p-out (p,p) polarization. The dashed line through the data represents only a guide to the eye.

Figure 2. SH rotational anisotropy from Ag(111) under p,p polarization conditions at the SH wavelengths indicated, for Ag(111) in UHV. The open circles represent the p-polarized SH data and theoretical fits using Equation 2 are indicated with a solid line. The fitted parameters $c^{(3)}/ a^{(\infty)}$ for each anisotropy are the following: (a) $1.2\, e^{i85^o}$; (b) $3.95\, e^{i81^o}$; (c) $1.74\, e^{i42^o}$; (d) 0.7 .

Figure 3. Wavelength dependence of the normalized SH intensity from Ag(111) (ϕ = 30°) in UHV for s-input and p-output (s,p) polarization as a function of the second harmonic photon wavelength in nm.

Figure 4. Wavelength dependence of the normalized SH intensity from Ag(111) (ϕ = 30°) in an electrolyte for p-input and s-output (p,s) polarization as a function of the second harmonic photon wavelength in nm (lower axis) and energy in eV (upper axis). The Ag(111) electrode was immersed in 0.1 M $NaClO_4$ and the electrode potential was held (a) at a positive bias, -0.2 V vs Ag/AgCl. (b) near the PZC, -0.7 V, and (c) at a negative bias, -1.2 V. The solid curve shown for each data set is a least squares fit to the Anderman model. (see text).

Figure 5. Imaginary part of the χ_{xxx} susceptibility (in arbitrary units), obtained from the fit of the spectra shown in Figures 4(a-c) to the Anderman model, plotted as a function of applied potential. The solid line through the points represents a linear least squares fit to the fitted parameter.

Figure 6. Wavelength dependence of the normalized SH intensity from a Ag(111) electrode ($\phi = 30^o$) under p,p polarization as a function of the second harmonic photon wavelength in nm (lower axis) and energy in eV (upper axis). The Ag(111) electrode was immersed in 0.1 M $NaClO_4$ and the electrode potential was held (a) at a positive bias, -0.2 V vs Ag/AgCl. (b) near the PZC, -0.7 V, and (c) at a negative bias, -1.2 V. The dashed line through each set of data represents only a guide to the eye.

Figure 7. Potential dependence of the SH rotational anisotropy from Ag(111) under m,s polarization conditions (under nonresonant conditions) at $2\lambda = 360$ nm. The Ag(111) electrode was immersed in 0.1 M $NaClO_4$ and the electrode potential was held (a) at a positive bias, -0.2 V vs Ag/AgCl, and (b) near the PZC, -0.7 V. The circles represent the s-polarized SH data and theoretical fits using Equation 5 are indicated with a solid line. The fitted parameters $c^{(3)}/ a^{(\infty)}$ for each anisotropy are the following: (a) 1.4 e^{i107^o}; (b) 3.1 e^{i99^o}.

Figure 8. Calculated magnitude of the Fresnel coefficients for the radiated SH light for the three different components of light, F_s (dotted line), F_k (dashed line) and F_z (solid line), as a function of the SH wavelength (nm) for an incidence angle of 30^o.

Figure 9. Results of a calculation of the binding energy of the n=0 surface state of Ag(111) as a function of the position of the image plane for -0.2 V (dashed curve, +0.5 V from the PZC), -0.7 V (solid curve, PZC) and -1.2 V (dotted curve, -0.5 V from the PZC). The

Fermi level is plotted as the vertical dashed line, and the solid horizontal line at $z_{im} = 0.21$ illustrates the intersection of these three curves with the image plane position determined by WHJ. From the figure, the intersection point determines the energetic position (with respect to e_f) of the n = 0 crystal-derived surface state at three values of the applied potential, -0.2 V (30 meV), -0.7 V (-30 meV), and -1.2 V (-85 meV).

Figure 1, Bradley et al.

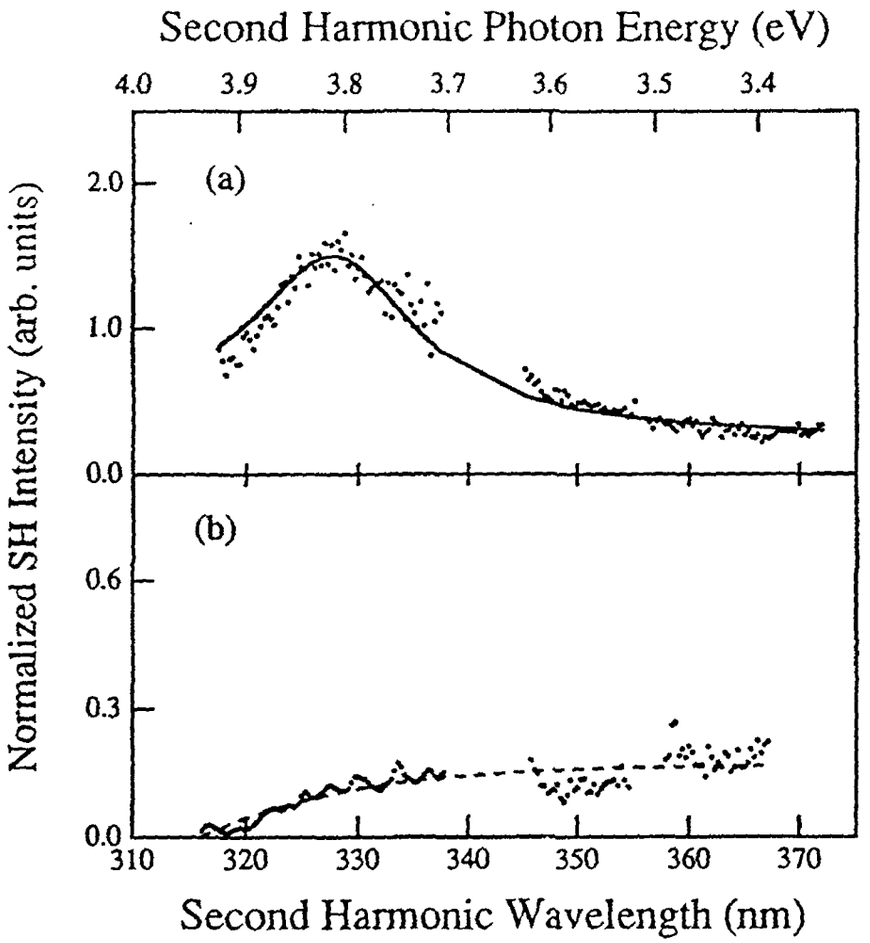

Figure 2, Bradley et al.

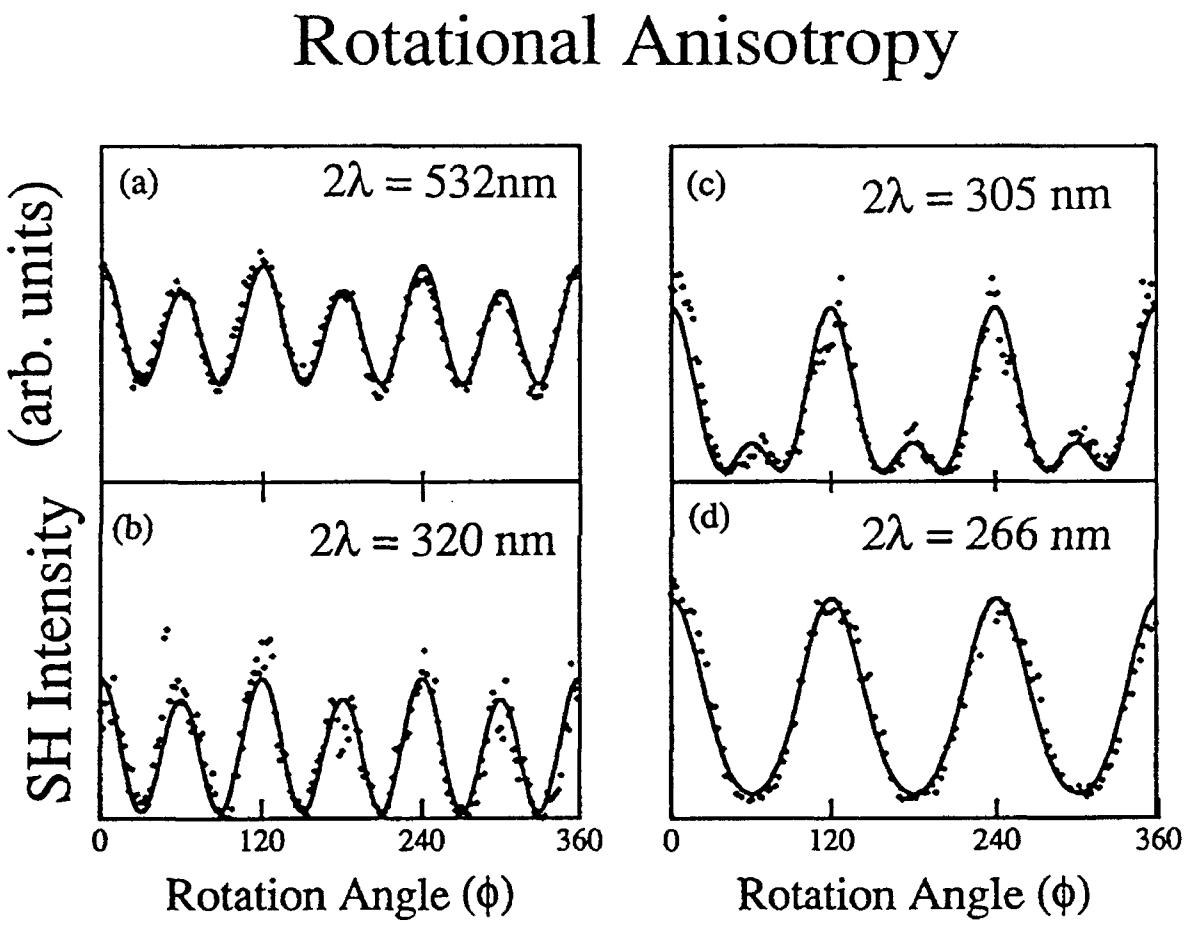

Figure 3, Bradley et al.

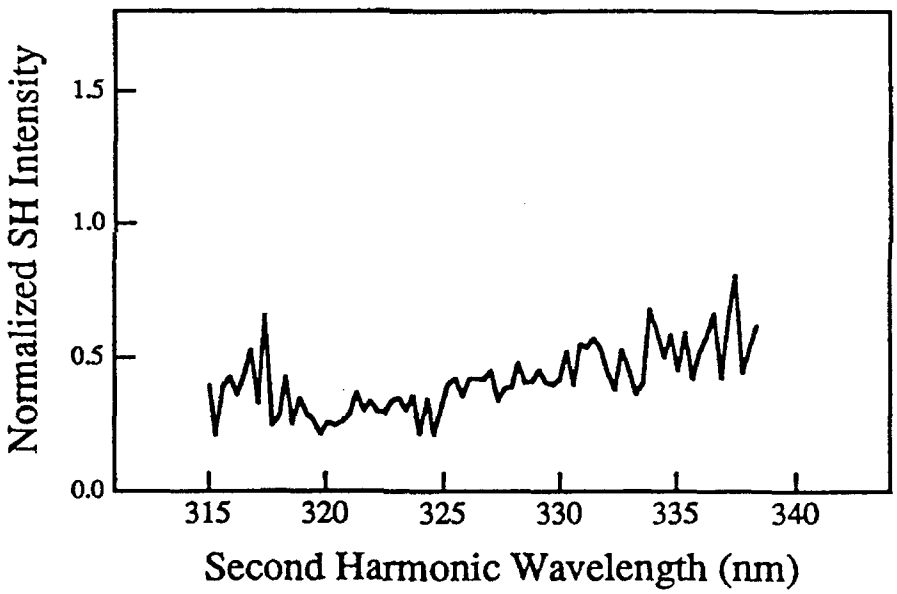

Figure 4, Bradley et al.

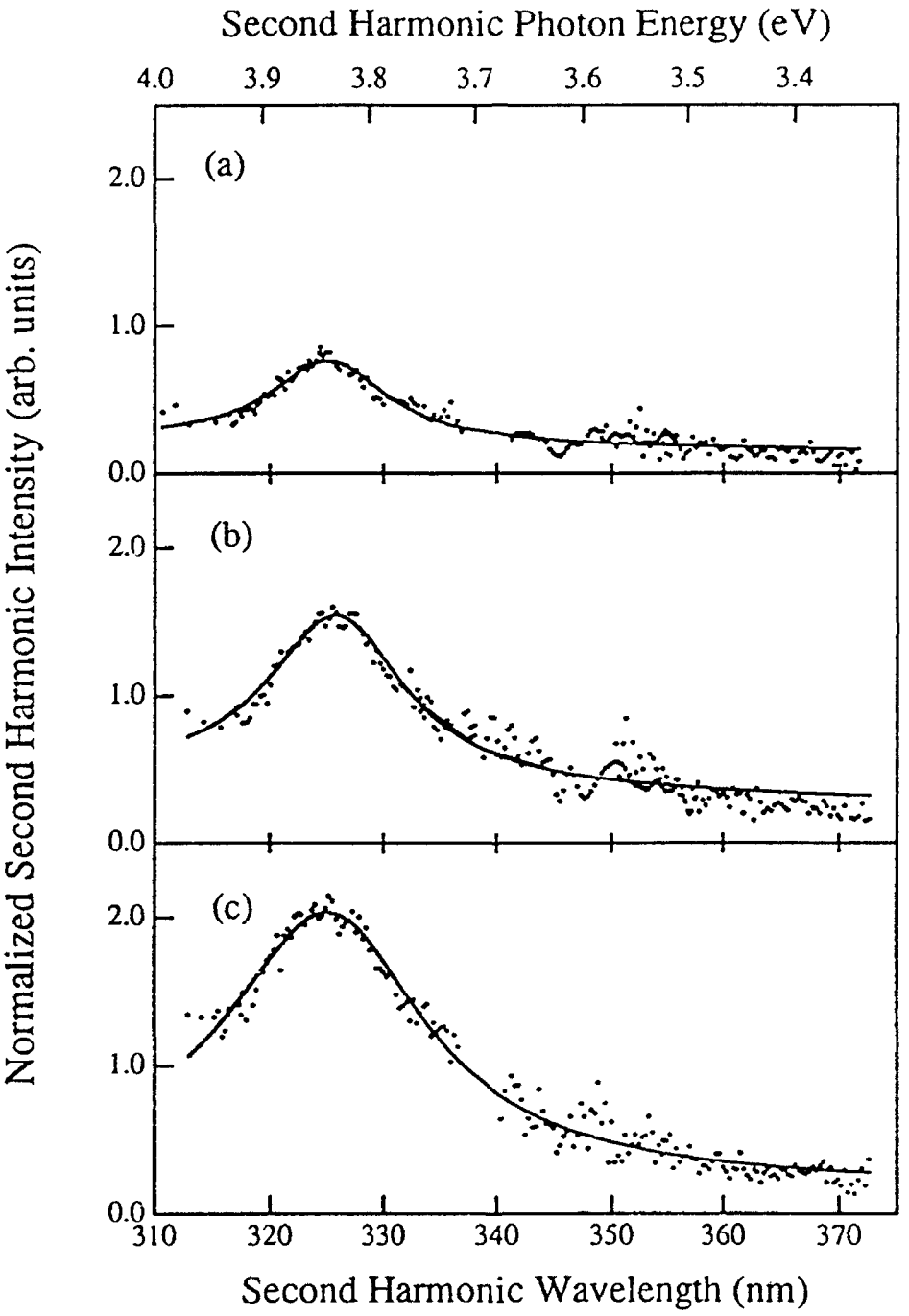

Figure 7, Bradley et al.

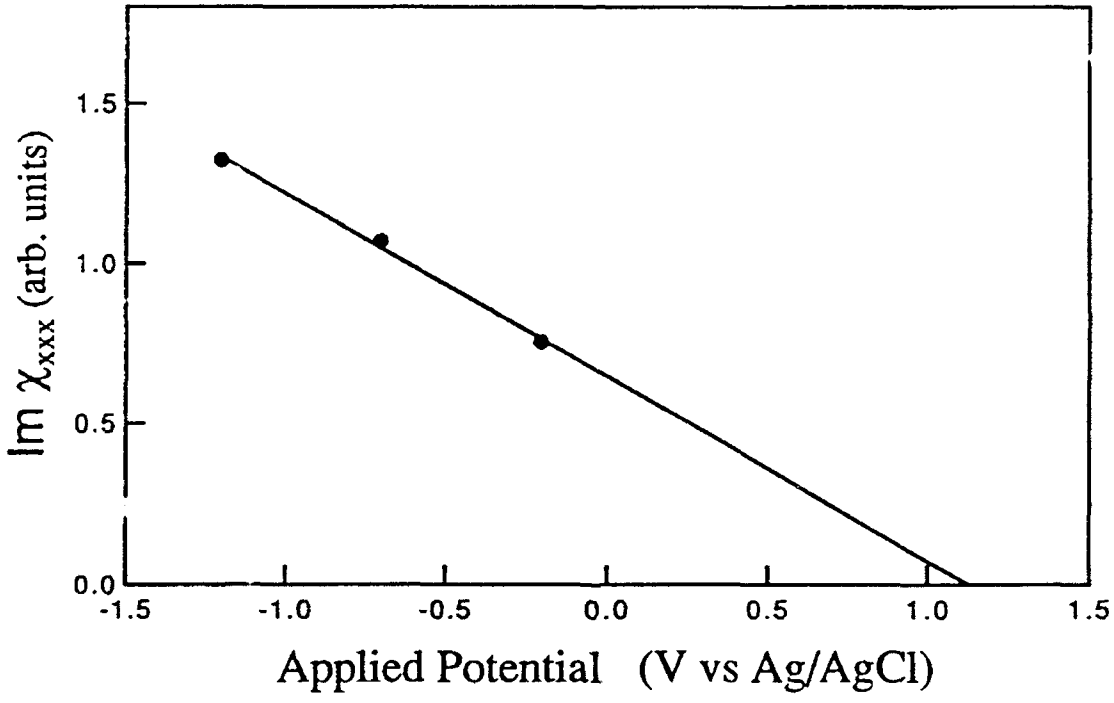

Figure 5, Bradley et al.

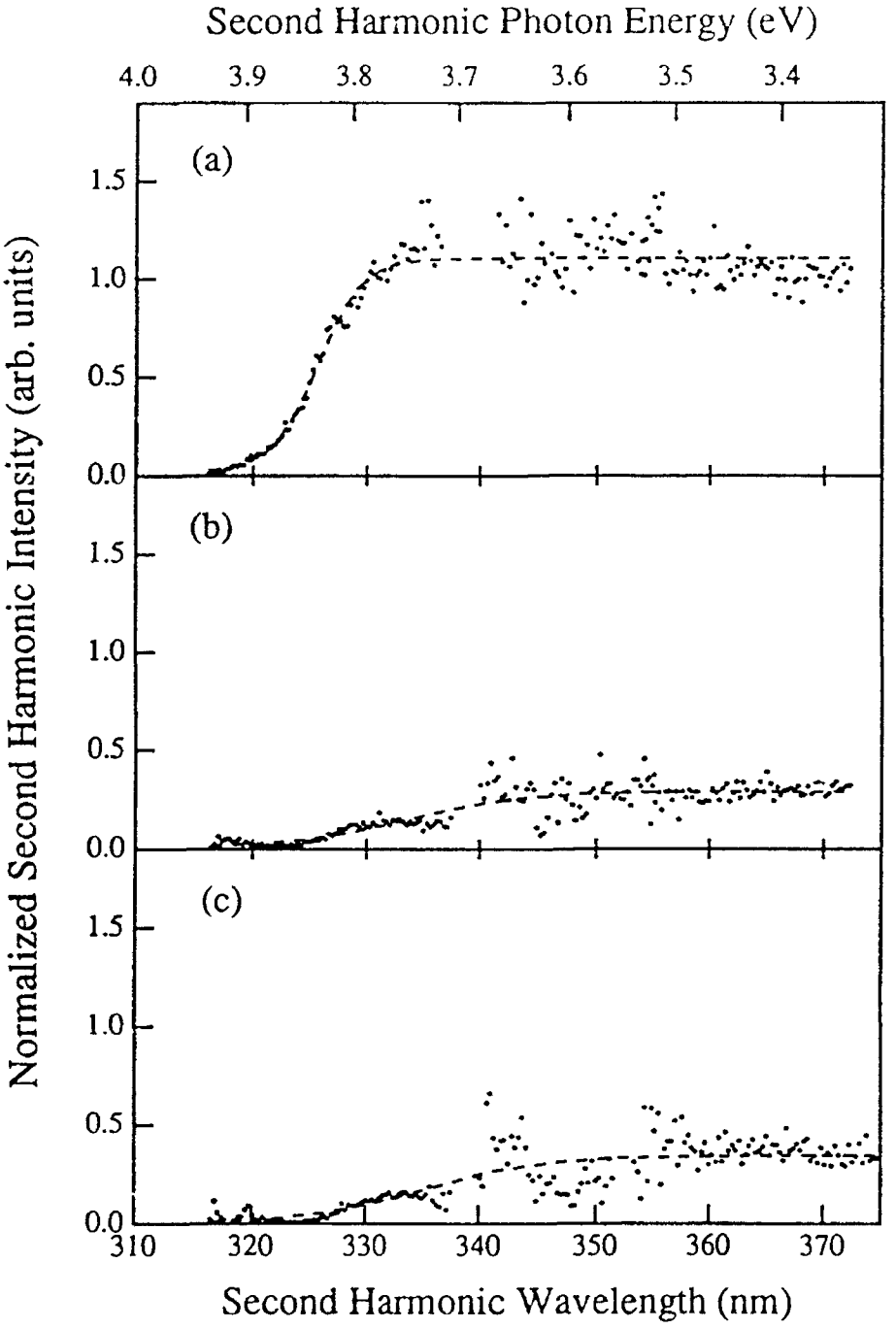

JCP Paper
Figures 7 (a,b)

Feb 1 Analysis

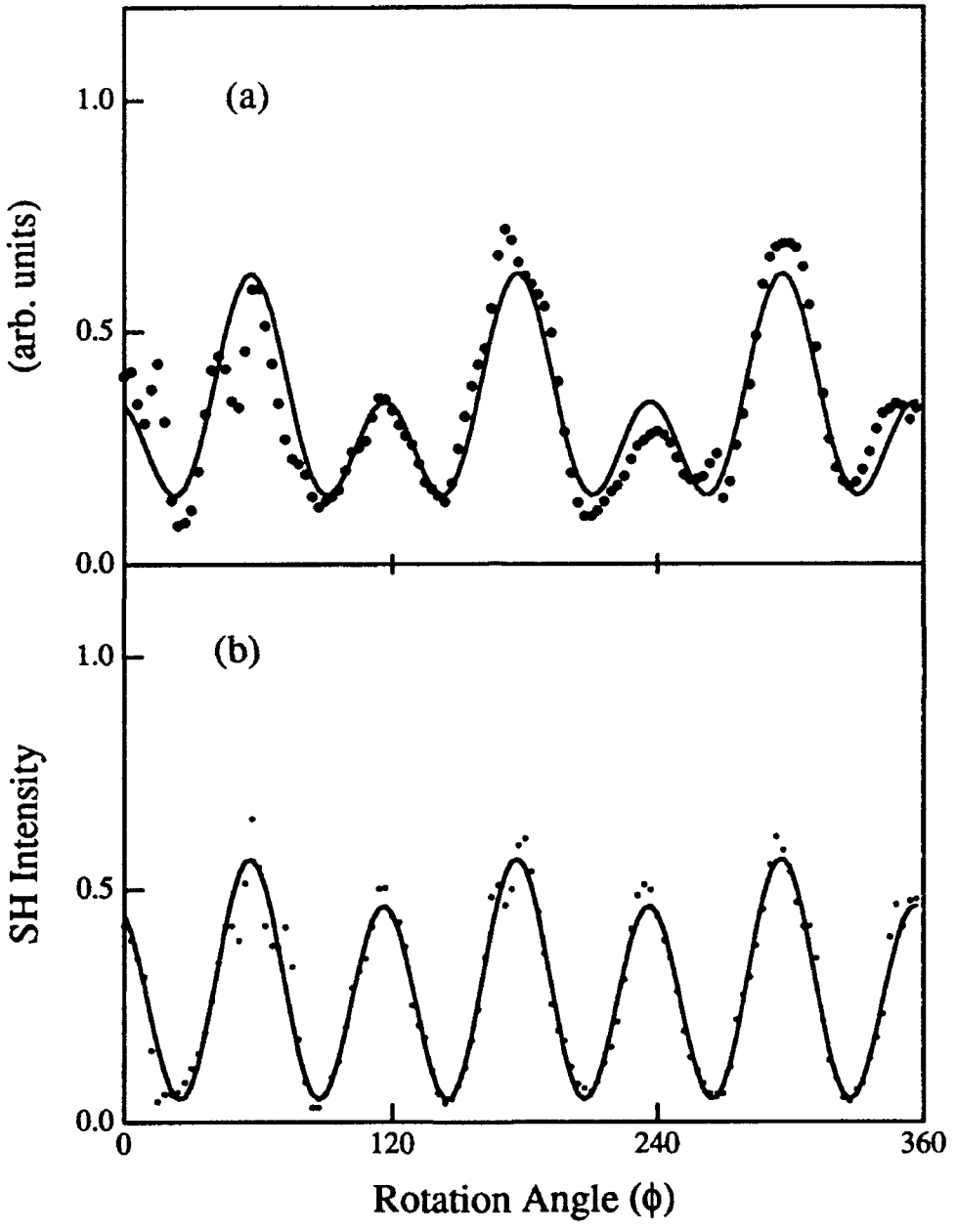

JCP Figure 8

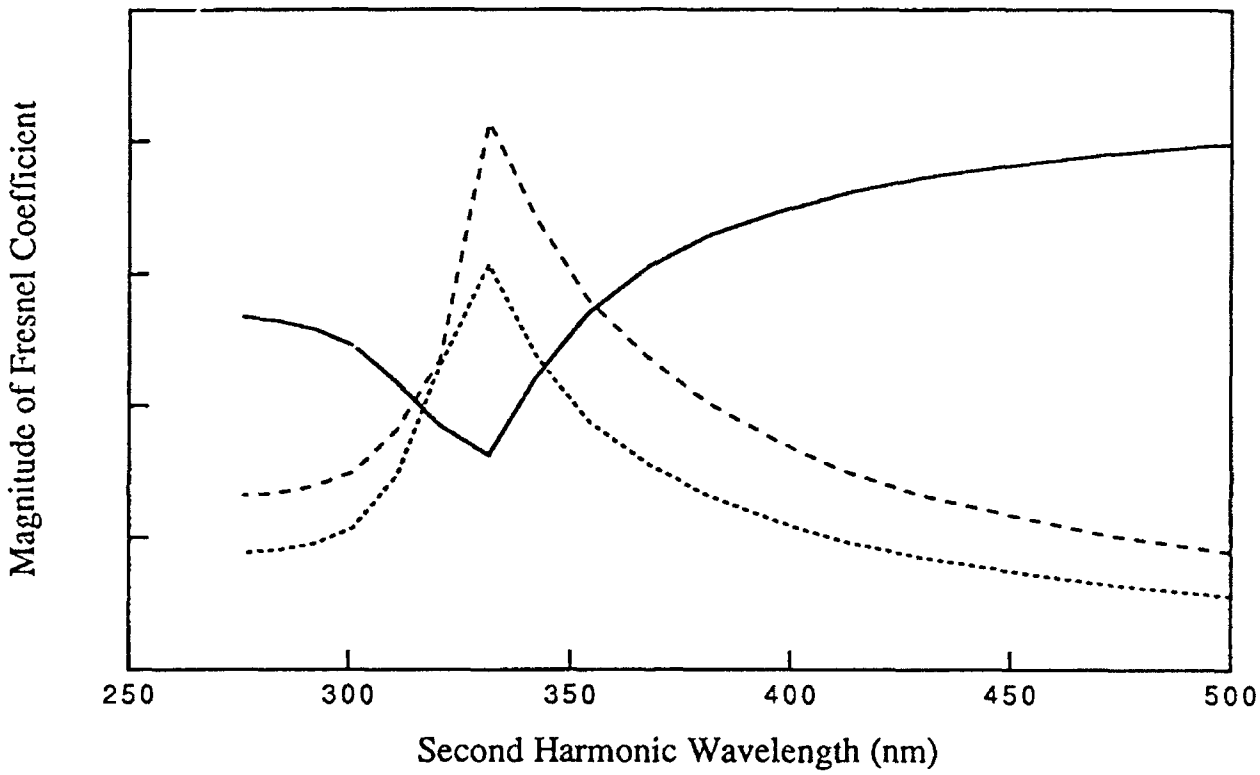
Magnitude of Fresnel Coefficient
250
300
350
400
450
500
Second Harmonic Wavelength (nm)

Figure 9

Figure 8, Bradley et al.